Supporting Information

Micromachined Multigroove Silicon ATR FT-IR Internal Reflection Elements for Chemical Imaging of Microfluidic Devices

Tyler A. Morhart[1,2], Stuart T. Read[2], Garth Wells[2], Michael Jacobs[2], Scott M. Rosendahl[2], Sven Achenbach[3] and Ian J. Burgess[1,§]

[1]Department of Chemistry, University of Saskatchewan, Saskatoon, Saskatchewan, S7N 5C9 Canada

[2]Canadian Light Source, Saskatoon, Saskatchewan, S7N 0X4 Canada

[3] Department of Electrical and Computer Engineering, University of Saskatchewan, Saskatoon, Saskatchewan, S7N 5A9 Canada

[*]corresponding author: email (ian.burgess@usask.ca)

Contents **Page**

Design and fabrication of the IR-compatible microfluidic device

Sampling in an attenuated total reflection (ATR) geometry offers a key advantage to working in transmission mode, namely that only solution which is within the penetration depth of the evanescent wave is sampled. In contrast, beams probing transmission devices will sample a pathlength at least equal to the resist thickness, so minimizing throughput losses demands the use of a thin resist. Such fabrication is technically challenging. With the ATR geometry there is no such requirement for thin resist and fabrication is less difficult. However, when spin-coating thick resists the small footprint of the micro-grooved Si IRE results in the formation of an edge bead which covers a large fraction of the IRE. Sealing such devices without additional steps to remove the edge bead was not possible. Instead, a negative tone dry resist (LamiRes_XP) was chosen as described in the main text. Laminating the resist from a film obviated the edge bead and was found to be much easier to seal.

Lamination was done by supporting the μ-groove IRE on an aluminum plate and placing a diced layer of LamiRes_XP on top, then covering the "sandwich" with a layer of overhead transparency. The IRE was oriented with the long axis of the grooves parallel to the feed direction. The rollers were about 100 mm in diameter. The rollers' large radius of curvature and the direction of the grooves prevented the IRE from breaking. In our hands, lamination had a 100% success rate for greater than 10 replicates.

UV laser exposure is described in the main text. After post-exposure bake and development, the device was sealed by a simple PMMA lid. The lid was cut from 3 mm thick stock to 9 x 11 mm^2 (the dimension of the microgrooved wafer) with a rotary tool. Three countersunk holes were machined using a 1.5 mm bit to form the through hole for liquid delivery followed by a 1/8" bit to form the countersink to a depth of about 1.5 mm. The countersink allowed the Tygon® tubing (OD = 1/8") to be dry-fitted before securing with Dymax 1142-M UV photoinitiated glue. Prior to sealing, a thin layer of Dymax 1142-M was spread with a razor blade on the lid. Then, the lid was carefully placed on the resist-coated IRE and the glue was allowed to spread by capillary forces along the resist/PMMA interface. The transparent PMMA allowed visual inspection of the progress of the glue spreading. The small amount of glue used afforded some time between complete spreading and infill into the microfluidic channel; in this time, the device was exposed using UV light point source at a distance of 10 cm for 10 s, after which the curing process was complete within a few seconds. After installation of tubing, inlet and outlet tubes were left at a length of about 10 cm for ease of portability. Connections to the pump and waste lines were made using press-fit 1/16" ID polypropylene unions (McMaster-Carr).

Illumination of the Focal Plane Array Detector

In order to determine how uniformly the FPA detector was illuminated, a Au-coated mirror was placed at the sample position and the reflected power was measured. Detector and collection settings were the same as those given in the main text. Figure S1 below shows representative data from the spectral region 3100 to 3200 cm^{-1}. In Figure S1a, the signal is calculated by integrating the single beam across the given spectral window. Detector illumination is relatively even and exhibits a slight decreasing gradient from bottom to top. The noise, shown in Figure S1b, was quantified by first subtracting a linear fit to the single beam across the spectral window then taking the standard deviation. Noise is almost completely uniform across the detector. The ratio of these two images forms Figure S1c, which shows the signal-to-noise ratio which is nearly constant across the detector area.

Other spectral regions are nearly identical and are not shown.

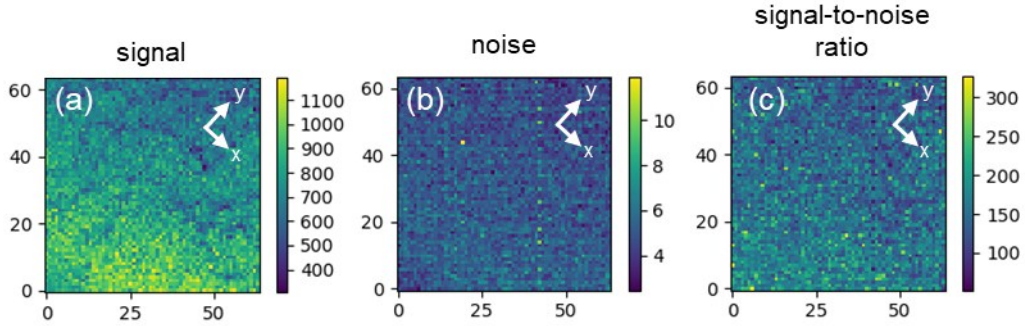

Figure S1. Illumination of the FPA detector by placing a mirror at sample. Numbers along horizontal and vertical axes indicate pixel number. a) Signal calculated from the integrated single beam spectrum in the chosen window. b) Standard deviation noise. c) Signal-to-noise ratio calculated by taking the ratio of the preceding two images. The uniform SNR shows that the globar evenly illuminates the detector.

Full Absorbance Image of the Checkerboard Pattern

Figure 4 in the main text presents a cropped and rotated image of the checkerboard pattern to facilitate interpretation. Here, the complete image is shown to demonstrate the limited area of the image which is well-focused. Figure S2 shows an absorbance image where the H_2O stretching mode is colour-mapped to blue. The rotation of the coordinate system is discussed in the main text and is imparted by the rotation angle between the collection mirror, M4, and the final mirror before the detector, M5.

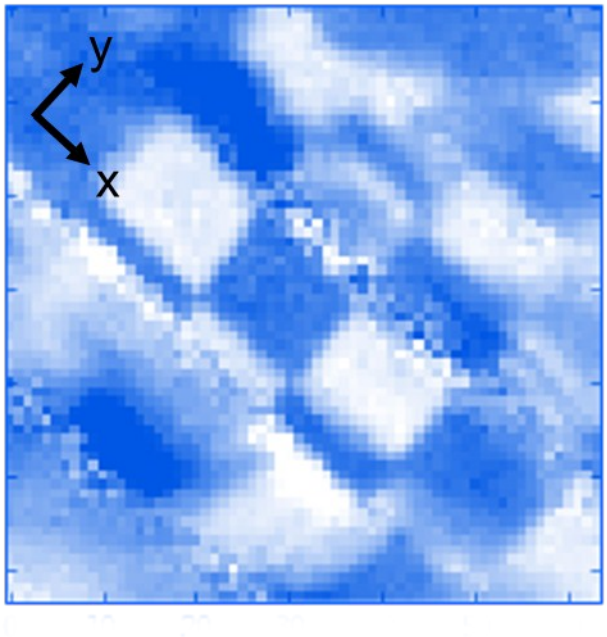

Figure S2. Full absorbance image of checkerboard pattern. Blue indicates the presence of water filling the voids. As discussed in the main text, only about 10% of the field of view is well-focused.

Composite Image of Co-Laminar Flow in the Microchannel

Similarly to Figure S2, below is shown the complete composite absorbance image of H_2O, D_2O, and HOD in the microchannel. A cropped and rotation portion of this image appears in Figure 6b of the main text.

The image shown is derived from a single hyperspectral image collected as per the Experimental section. Three separate images were created by integrating characteristic absorption bands for each of the three species present in the channel. Each of these images was thresholded. Then, the three images were colour-mapped to indicate which chemical species they measured and overlaid as shown below.

As discussed previously, only a narrow diagonal stripe is well-focused; that portion is shown in Figure 7b, and it is bounded by two diagonal slashes which correspond to noise in the constituent images.

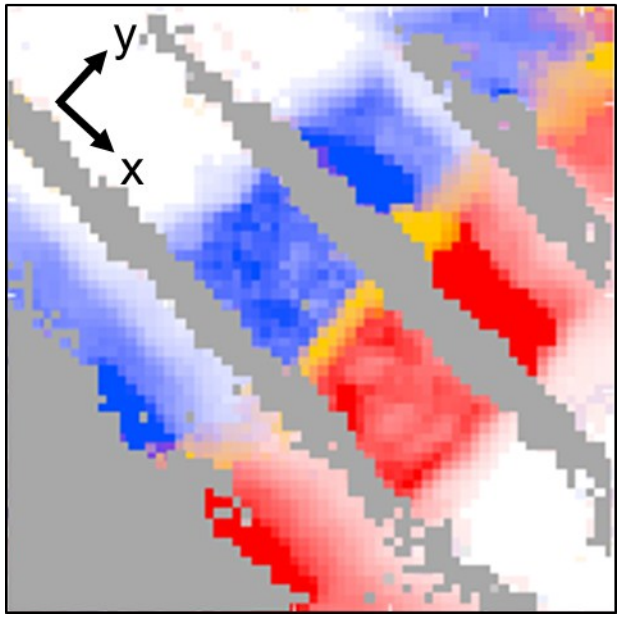

Figure S3. Full composite absorbance image of co-laminar flow in the microchannel. H_2O is mapped to blue, D_2O to red, and HOD to orange. Pixels with no analytical signal have been mapped to grey.

Composite Image including Photoresist

As described in the main text, the microchannel was measured by optical microscopy to be 505 μm wide. However, the composite chemical absorbance image shown as part of Figure 6 shows that the integrated absorbance of H_2O or D_2O is broadened from the step function that is expected. The explanation in the text is that partial delamination of the resist occurs at the edges, allowing some fluid to seep underneath. Overlaying the absorbance from the photoresist over Figure 6b provides additional evidence.

The photoresist integrated absorbance, shown in violet in Figure S4, was calculated by integrating a characteristic absorption at 1184 cm^{-1}. Because the absorbance images used in the main text effectively cancel out the contributions from the photoresist, this band was chosen because it is strong enough to be visible in the single beam spectra and does not overlap with any other bands. For each pixel, the band was integrated in the single beam and normalized to the integral of the entire single beam to correct for differing pixel intensities.

In the image below, the width of the channel is 515 μm which is identical within FPA pixel resolution to that measured by optical microscopy. A mild gradient (light to dark violet) of photoresist absorption can be observed at the extremes of the channel. This matches well with that observed in Figure 6, indicating that the resist has lifted at the edges.

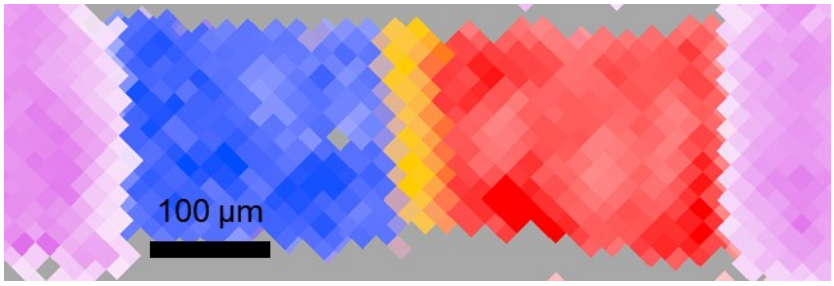

Figure S4. Composite absorbance image with photoresist absorbance signal overlaid in violet.

Geometric Ray Tracing

Two-dimensional geometric ray tracing was performed with OptGeo software (version 2.24) available at http://jeanmarie.biansan.free.fr/optgeo.html. The refractive index of the μ-groove Si IRE was set to 3.4 and monochromatic light was used.